Journal of Inorganic Biochemistry 114 (2012) 8–14

Contents lists available at SciVerse ScienceDirect

Journal of Inorganic Biochemistry

journal homepage: www.elsevier.com/locate/jinorgbio

Overexpression, purification, and biochemical and spectroscopic characterization of copper-containing nitrite reductase from *Sinorhizobium meliloti* 2011. Study of the interaction of the catalytic copper center with nitrite and NO

Félix M. Ferroni [a], Sergio A. Guerrero [b], Alberto C. Rizzi [a], Carlos D. Brondino [a,*]

[a] Departamento de Física, Facultad de Bioquímica y Ciencias Biológicas, Universidad Nacional del Litoral, Ciudad Universitaria, Paraje El Pozo, S3000ZAA Santa Fe, Argentina
[b] Laboratorio de Bioquímica Microbiana, Instituto de Agrobiotecnología del Litoral (CONICET-UNL), Ciudad Universitaria, Paraje El Pozo, S3000ZAA Santa Fe, Argentina

ARTICLE INFO

Article history:
Received 5 December 2011
Received in revised form 23 April 2012
Accepted 24 April 2012
Available online 3 May 2012

Keywords:
Nitrite reductase
Copper
Sinorhizobium meliloti
Rhizobacteria
Nitrogen metabolism
EPR

ABSTRACT

The entire *nirK* gene coding for a putative copper-nitrite reductase (Nir) from *Sinorhizobium meliloti* 2011 (*Sm*) was cloned and overexpressed heterologously in *Escherichia coli* for the first time. The spectroscopic and molecular properties of the enzyme indicate that *Sm*Nir is a green Nir with homotrimeric structure (42.5 kDa/subunit) containing two copper atoms per monomer, one of type 1 and the other of type 2. *Sm*Nir follows a Michaelis–Menten mechanism and is inhibited by cyanide. EPR spectra of the as-purified enzyme exhibit two magnetically different components associated with type 1 and type 2 copper centers in a 1:1 ratio. EPR characterization of the copper species obtained upon interaction of *Sm*Nir with nitrite, and catalytically-generated and exogenous NO reveals the formation of a Cu-NO EPR active species not detected before in closely related Nirs.

1. Introduction

Denitrification constitutes one of the three main branches of the biogeochemical nitrogen cycle performed by bacteria [1,2]. This branch involves the sequential reduction of nitrate to dinitrogen by means of four enzymes with different structural properties and cell localization. Distinct types of microorganisms were shown to have the machinery to perform this process. Some of them, as is the case of rhizobia which live symbiotically in root nodules of legumes, are widely used in agriculture because of their ability to take dinitrogen from the atmosphere [3], but in parallel may produce negative impacts in the environment because they can produce the greenhouse gas N_2O and acidification of soils [4–6].

Nitrite reductase is the enzyme that catalyzes the second step of the denitrifying pathway according to the reaction

$$NO_2^- + 2H^+ + e^- \rightarrow NO + H_2O \quad E^\circ = 370\,mV$$

In denitrifying bacteria this reaction can be catalyzed by two nitrite reductases, one containing a cd_1 heme and the other containing copper, which are produced by the structural genes *nirS* and *nirK*, respectively [1,7]. Copper-containing nitrite reductase (Nir) presents homotrimeric structure (~40 kDa/monomer) with two copper atoms per monomer [8–10], one of type 1 (T1, also blue copper) and the other of type 2 (T2, also normal copper). Nirs have been classified into two groups according to the UV–visible (UV–vis) properties of their T1 centers. Blue Nirs (*e.g.* from *Pseudomonas aureofaciens* and *Alcaligenes xylosoxidans*) exhibit a very intense absorption band at ~590 nm, whereas green Nirs (*e.g.* from *Achromobacter cycloclastes* and *Alcaligenes faecalis*) present two intense absorption bands at ~460 and 600 nm [1]. The T1 Cu is coordinated by two histidine imidazoles, a cysteine thiolate, and a methionine thioether in an axially flattened tetrahedron in green Nirs or in an axially distorted tetrahedron in blue Nirs [10,11]. The difference in color was shown to be produced by the geometrical distortion of the T1 center [12]. The T2 site shows a distorted tetrahedral geometry with a water molecule and three histidine residues, two from one monomer and another from the adjacent monomer. T1 is an electron transfer center [13], whereas T2 is the catalytic center [14]. T1 and T2 are ~12 Å apart bridged by a histidine-cysteine pathway proposed to be involved in electron transfer. The proposed reaction mechanism implies that nitrite binds to the T2 center and is converted to NO by reducing equivalents delivered by the T1 center through the bridging chemical path. Regarding the reaction mechanism, there is a controversy in relation to what process occurs first: nitrite binds to the oxidized T2 center after which an electron is transferred from the T1 to the T2 center, or the T2 center is first reduced followed by nitrite binding [15,16].

Sinorhizobium meliloti is a nitrogen fixing bacterium belonging to rhizobia that forms symbiotic relationships with legumes like alfalfa (*Medicago sativa*) [3]. *S. meliloti* 1021, a streptomycin-resistant derivative

* Corresponding author. Tel.: +54 342 4575213; fax: +54 342 4575221.
E-mail address: brondino@fbcb.unl.edu.ar (C.D. Brondino).

0162-0134/$ – see front matter © 2012 Elsevier Inc. All rights reserved.
doi:10.1016/j.jinorgbio.2012.04.016

of wild type *S. meliloti* 2011, is the only strain of the genus *Sinorhizobium*, family Rhizobiaceae, order Rhizobiales whose genome sequence has been reported [17–20]. The genome sequence of *S. meliloti* 1021 encodes for several putative nitrogen metabolism-related proteins. As part of our work devoted to characterize denitrifying metalloenzymes in rhizobia, we report a rapid high-yield heterologous expression, a purification protocol, and molecular, kinetic, and spectroscopic properties of the putative nitrite reductase encoded by the *nirK* gene (SMa1250) in the nitrogen fixing bacterium *S. meliloti* 2011. The characterization of the copper species obtained upon interaction of *Sm*Nir with nitrite reveals the formation of an EPR active species not detected before in closely related Nirs.

2. Materials and methods

2.1. Growth conditions and DNA extraction

Sm cells obtained from 5 mL of an overnight YME standing culture at 30 °C were collected by centrifugation at 6000 rpm and washed three times with 100 mM Tris–HCl buffer pH 8.0. Cells were resuspended in 750 μL of 100 mM Tris–HCl buffer pH 8.0 and incubated for 2 h at 37 °C with 40 μL of lysozyme (13 mg mL^{-1}, Fluka). Then, the mixture was incubated for 2 h at 56 °C after addition of 40 μL of 10% SDS and of 20 μL of Proteinase K (20 mg mL^{-1}, Genbiotech).

The cell lysate was subjected to deproteinization with phenol. The mixture was treated with 400 μL of phenol-saturated 100 mM Tris–HCl buffer pH 8.0 and centrifuged at 13,000 rpm for 30 min. The aqueous phase was treated with 200 μL of phenol-saturated 100 mM Tris–HCl buffer pH 8.0 and 200 μL of chloroform-isoamyl alcohol (24:1) and centrifuged at 13,000 rpm for 5 min. The last step was performed twice. Finally, the supernatant was treated with 0.1 volumes of 3 M sodium acetate pH 6.5 and 2 volumes of ice-chilled ethanol. This mixture was kept at −20 °C for 2 h and centrifuged for 30 min at 15,000 rpm and 10 °C. The pellet was washed with 70% ethanol and centrifuged at 10,000 rpm for 15 min. The pellet was dried at 37 °C and dissolved in 100 μL of TE buffer. The DNA solution was stored at −20 °C.

2.2. Cloning of the nirK gene

Based on information obtained from the reported *S. meliloti* 1021 genome sequence (SMa1250, http://genome.kazusa.or.jp/rhizobase/sinorhizobium), two specific oligonucleotides were designed to amplify *nirK*. The sequence of the cloned gene encodes a product with a signal peptide directing the protein to the periplasm. In order to facilitate the further subcloning in the expression vector, the primers were designed including the restriction sites Nde I (in forward primer, Fw: 5′-CATATGTCTGAGCAATTCCAG-3′) and Sac I (in reverse primer, Rv: 5′-GAGCTCTCAGGTGCCCGAAGG-3′). PCR was performed with 20 pmol of each primer, 1 ng of DNA, 1 unit of *Pfu* DNA polymerase (Genbiotech), 2 μL of PCR reaction buffer (Genbiotech), 0.2 mM dNTPs (Genbiotech) and 1 mM $MgCl_2$ in 20 μL of reaction volume. The PCR reaction was performed in an Eppendorf thermocycler using the following program: 5 min at 94 °C, 30 cycles of 1 min at 94 °C, 30 s at 55 °C, and 2 min at 72 °C, and a final elongation at 72 °C for 10 min.

The purified PCR product was cloned into the pJET1.2/blunt cloning vector (Fermentas) using the CloneJET™ PCR cloning kit (Fermentas). The ligation mixture was used to transform *Escherichia coli* TOP10 competent cells (Invitrogen Corp., Carsbad, CA, USA) and to select positive clones in LB-Ampicillin plates (100 μg mL^{-1}). The plasmid pJSK (4105 bp) was digested with FauND I (Nde I, Genbiotech) and Sac I (Fermentas) and the released Nde I/Sac I-insert was ligated into purified FauND I_Sac I-digested pET22b(+) (Novagen) to obtain p22SK expression constructs. The p22SK plasmids were used to transform *E. coli* BL21(DE3) cells.

Plasmids purifications were performed using the JET Quick plasmid miniprep spin kit (Genomed). The PCR and plasmid digestions products were purified from agarose gel using the AccuPrep® Gel Purification Kit (Bioneer). The fidelity of the inserted sequences of pJSK constructs was verified by sequencing using the Sanger method [21].

2.3. Overexpression and purification

Overexpression of the *nirK* gene was achieved by introducing p22SK into *E. coli* BL21 (DE3). The transformed strain was grown aerobically at 30 °C with agitation at 200 rpm to an A_{600} of ~0.6 in Lysogeny broth supplemented with 0.6 mM $CuSO_4$. Next, the induction was performed by adding 0.2 mM Isopropyl-β-D-1-thiogalactopyranoside (IPTG) and the cells were allowed to grow for 2.5 h at 200 rpm. Cells were then harvested by centrifugation at 3800×*g* for 20 min, resuspended in 20 mM Tris–HCl buffer pH 6.0, and disrupted by sonication. The crude extract was recovered by centrifugation at 25,000×*g* for 1 h and dialyzed for 4 h against 20 mM Tris–HCl buffer pH 6.0 supplemented with 0.6 mM $CuSO_4$ and then centrifuged at 25,000 ×*g* for 1 h. *Sm*Nir from the crude extract was purified in a single chromatographic step. The crude extract was loaded onto a Source 15Q matrix column (1.6×13 cm, GE Pharmacia Biotech AB) equilibrated with 20 mM Tris–HCl pH 6.0. *Sm*Nir appeared as an intense green band at the top of the column. Unbound proteins were removed by washing the column with 2 volumes of 50 mM NaCl in 20 mM Tris–HCl buffer pH 6.0. Bound proteins were eluted applying a linear gradient in equilibration buffer (50 to 600 mM NaCl in 20 mM Tris–HCl buffer pH 6.0, 5 volumes). The pure *Sm*Nir fraction was pooled and dialyzed against 100 mM Tris–HCl buffer pH 6.0. Finally, *Sm*Nir was concentrated to approximately 18 mg mL^{-1} by an Amicon Ultra 30 K NMWL device and stored at −80 °C. Protein purity was evaluated by SDS-PAGE.

2.4. Protein quantification, molecular mass, and N-terminal amino acid sequence determination

Molecular properties were determined in both cytoplasmic and periplasmic fractions, which were obtained following a procedure reported elsewhere [22]. Protein concentration was determined using the Bradford method with bovine serum albumin as standard [23]. The molecular mass of the as-isolated enzyme was estimated by gel filtration chromatography. A prepacked Superdex 200 HR 10/30 column (GE Healthcare) connected to a high performance liquid chromatography device (Akta basic, GE Healthcare) was equilibrated with 300 mM Tris–HCl buffer, pH 7.6 with 0.2% (v/v) Tween 80. Isocratic elution at a flow rate of 0.4 mL min^{-1} was performed with detection at 280 nm. The molecular mass markers used for calibration were ferritin (440 kDa), alcohol dehydrogenase (150 kDa), bovine serum albumin (66 kDa) and carbonic anhydrase (29 kDa), all from GE Healthcare. The molecular mass of the subunits was estimated by SDS-PAGE according to the method of Laemmli [24]. Samples were loaded onto a 12% denaturing poliacrylamide gel after treatment with SDS-PAGE sample buffer for 30 min at 45 °C. The molecular weight markers (GE Healthcare) for calibration were phosphorylase *b* (97.0 kDa), albumin (66.0 kDa), ovalbumin (45.0 kDa), carbonic anhydrase (30.0 kDa), trypsin inhibitor (20.1 kDa) and α-lactalbumin (14.4 kDa). The N-terminal amino acid sequence was determined by the Edman degradation method [25] on an Applied Biosystems 477A sequencer.

2.5. Activity assays

Kinetic studies and activity screening were performed using the method described by Ida with some modifications [26]. Enzyme activity assays were performed in a reaction mixture containing 30 mM sodium phosphate buffer pH 7.0, 0.3 mM methyl viologen, enzyme (0.8 μg/mL) and variable sodium nitrite concentration in the 50–5000 μM range. The reaction was started by addition of 5 mM sodium dithionite to a final volume of 250 μL. After 10–20 min at 30 °C, the reaction was stopped by vigorously shaking to oxidize the excess reductant. The

remaining nitrite was detected by the diazo-coupling method [27]. Absorbance at 540 nm was measured after 10–20 min incubation (linear response was checked). One unit of activity (U) corresponds to the reduction of 1 μmol of NO_2^- min^{-1}. The specific activity was measured in nmol NO_2^- min^{-1} mg^{-1} protein. Kinetic data were analyzed by least square fitting the data to a Michaelis–Menten model.

Alternatively, *Sm*Nir enzyme activity was measured with a continuous spectrophotometric assay that uses dithionite as the sole electron donor [28,29]. The reaction mixture contained 1 mM sodium dithionite, 250 μM nitrite, and 72 μg of enzyme in a final volume of 700 μL. The reaction was started by adding either nitrite or dithionite under anaerobic conditions, after which the oxidation rate of dithionite was followed spectrophotometrically at 315 nm. This method was used to evaluate the optimum pH of enzyme activity. The pH range assayed was 5 to 9. The data were corrected for the chemical reduction of nitrite observed below pH 6. The influence of the reactants addition order was checked at pH 7.

Sodium azide (25 mM), potassium cyanide (1 mM), sodium nitrate (1 mM), and ammonium chloride (1 mM) were tested as inhibitors. *Sm*Nir samples were incubated previously to the enzymatic assay with each inhibitor at 4 °C for 10 min and followed with the diazo-coupling method under the same experimental conditions as those used in the enzyme activity assay.

2.6. Metal analysis

Copper contents were determined by atomic absorption spectrometry using a Perkin Elmer Analyst 800 spectrometer.

2.7. Spectroscopic methods

UV–vis spectra were recorded on a Perkin Elmer Lambda 20 UV–vis spectrophotometer.

EPR measurements were performed at X-band on a Bruker EMX Plus spectrometer equipped with a universal high sensitivity cavity (HSW10819 model) and an Oxford Instruments helium continuous-flow cryostat. Spectra were acquired under non-saturating conditions. Experimental: microwave frequency, 9.26 GHz; modulation field, 100 kHz; modulation amplitude, 2 G; microwave power, 0.2 mW; temperature, 60 K. EPR spectra were simulated with the EasySpin toolbox based on MATLAB® [30]. Spectra taken in the temperature range 20–200 K showed no significant differences.

Samples for EPR spectroscopy were concentrated to ~150 μM trimeric protein by an Amicon concentrator. Degassed solutions of ascorbate, dithionite, and NO were withdrawn by gastight syringe from the vessels containing the respective solutions and loaded into argon-flushed EPR

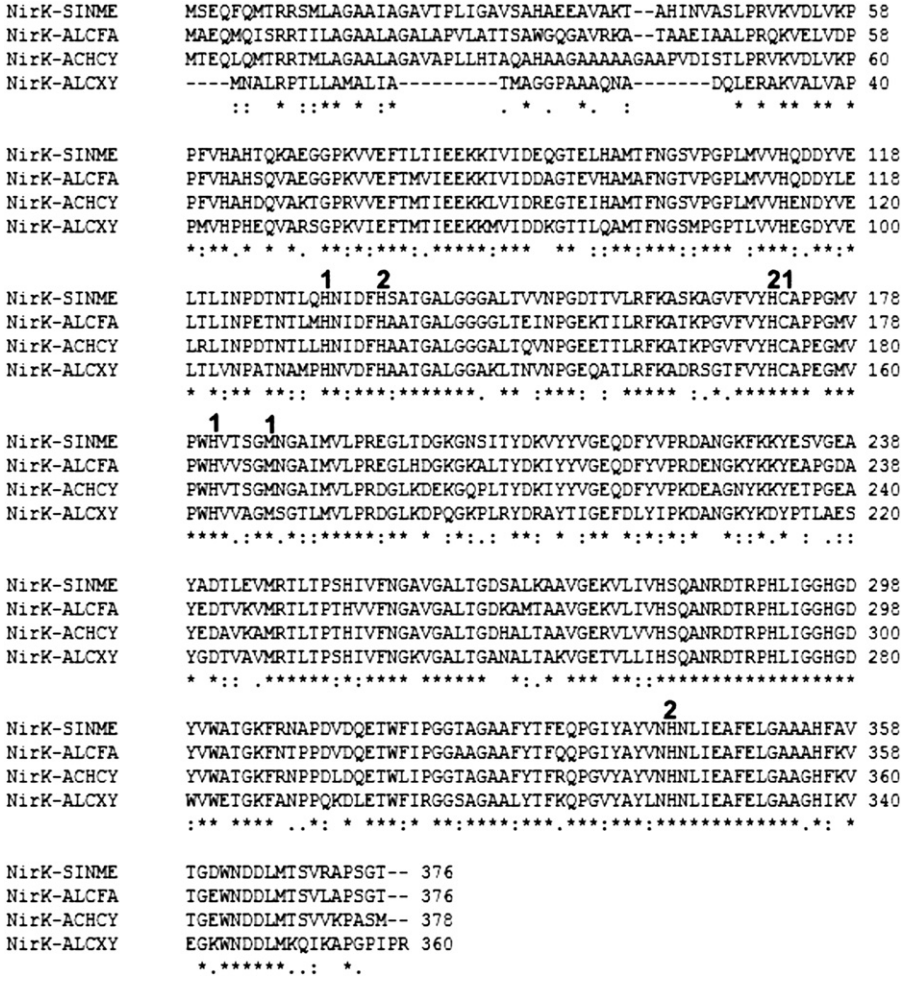

Fig. 1. Alignment of the deduced amino acid sequences of copper-containing nitrite reductases from different bacterial sources. The amino acid alignment was obtained with the Clustal W program [53]. Identities are shown with asterisks and similarities with single dots. The numbers 1 and 2 above the sequence alignment indicate the T1 and T2 copper ligands, respectively. SINME, *S. meliloti*; ALCFA, *A. faecalis*; ACHCY, *A. cycloclastes*; ALCXY, *A. xylosoxidans*. Nirs from ALCFA and ACHCY are green, whereas that from ALCXY is blue.

tubes containing samples of *Sm*Nir (~200 μL) followed by gentle mixing. The EPR tubes were frozen with liquid nitrogen and kept under these conditions until use. The saturated solution of NO was generated by dropwise addition of a solution of 500 mg of $NaNO_2$ in 8 mL of degassed water to a solution containing 2.2 g of $FeSO_4.7H_2O$, 1 mL of concentrated H_2SO_4 in 15 mL of degassed water. The generated NO was passed through a 1 M KOH solution to remove higher oxides.

3. Results and discussion

3.1. Cloning and expression of nirK gene

The entire *nirK* gene (SMa1250) coding for a putative copper-nitrite reductase was cloned and overexpressed in *E. coli*. Overproduction of the enzyme in *E. coli* BL21(DE3) [p22SK] was optimized on a small scale (5–10 mL culture) by testing different growth temperature, IPTG concentration, and induction time. Optimal conditions were $T = 30$ °C, 0.2 mM IPTG, and 2.5 h of induction. Higher IPTG concentrations and temperatures yielded protein aggregates as inclusion bodies. The enzyme purification is rapid involving one step procedure that can be completed in one day.

The N-terminal regions were determined for polypeptides obtained from periplasm and cytoplasm. Periplasmic polypeptides showed the LIGAVS, AAIAGA, GAVTPL and AGAAIA sequences, whereas those isolated from cytoplasm showed the SEQFQM and LIGAVS sequences (Fig. 1). Sequence analysis confirms that all these polypeptide sequences correspond to the product of *Sm nirK* gene, although with some degree of proteolysis. This phenomenon is not new as several Cu-containing Nirs showed proteolytic degradation at the N-terminus depending on the purification procedure [31,32]. Furthermore, the mature *Sm*Nir was slightly different from that predicted by the SignalP program [33,34], since the cleavage site is predicted to be between 33 and 34 amino acid positions (AHA↓EE , see Fig. 1).

Alignment of the deduced amino acid sequences of *Sm*Nir and Nirs from other sources is also shown in Fig. 1. *Sm*Nir exhibits 79 and 82% overall sequence identity with the green Nirs from *A. faecalis* and *A. cycloclastes*, respectively, and 65% overall sequence identity with the blue Nir from *A. xylosoxidans*, suggesting that *Sm*Nir belongs to the green-type Nirs, a result in line with the UV–vis spectroscopy (see below).

The copper centers appear to be rather unstable and may be lost during the purification procedure, decreasing the enzyme specific activity. Copper addition to the crude extract increased the specific activity of the wild type *A. xylosoxidans* Nir approximately 15 times [35,36]. A recombinant Nir from *Rhodobacter sphaeroides* 2.4.3 containing no copper was reported, and the full metal content could be recovered by adding copper to the apoprotein [37]. Our results showed considerable Nir activity levels in the crude extract (62 U mg of protein^{-1}) obtained from a medium amended with copper. This enzyme activity levels increased 1.6 times by dialysis with a copper solution prior to purification and the color of the crude extract turned from yellow to green after dialysis, in line with the above mentioned examples.

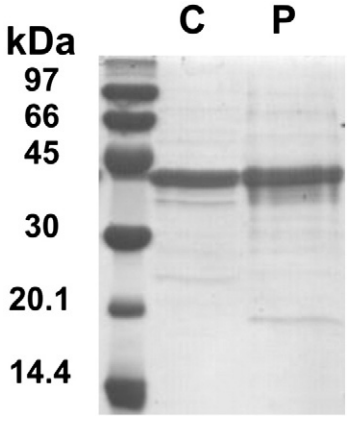

Fig. 2. SDS-PAGE of *Sm*Nir. Molecular mass markers in kDa (GE Healthcare); C and P correspond to fractions purified from cytoplasm and periplasm, respectively.

3.2. Molecular properties and UV–vis spectra

Molecular mass determination by gel filtration of *Sm*Nir from both cytoplasmic and periplasmic fractions yielded a value of ~127 kDa, whereas SDS-PAGE showed a unique band with molecular mass of ~42.5 kDa (Fig. 2). This indicates a trimeric structure, as observed in Nirs from other sources [1,7].

Metal analysis identified 5.9 ± 0.1 Cu/trimer, in agreement with the values expected for Nir enzymes having fully occupied T1 and T2 copper sites.

Fig. 3 shows the UV–vis spectra of *Sm*Nir under different experimental conditions. The spectrum of the as-purified enzyme (spectrum a) shows absorption maxima at 456 nm (9.1 $mM^{-1}\,cm^{-1}$) and 586 nm (7.6 $mM^{-1}\,cm^{-1}$), bands typical of green T1 copper sites [1].

The addition of sodium ascorbate or sodium dithionite led to the disappearance of all visible bands (Fig. 3, spectrum b), consistent with a T1 center in its reduced form. The low intensity absorption at 412 nm is likely a small cytochrome contamination, estimated to be less than 2% of the total protein. Sodium nitrite addition to ascorbate- and dithionite-reduced *Sm*Nir under argon atmosphere restored all the bands observed in the as-purified form but with lower intensity (Fig. 3, spectrum c), indicating a partial oxidation to Cu(II) of T1. This experimental evidence indicates that T1 copper site oxidation is via an electron transfer between T1 and T2, since the enzyme-nitrite interaction is known to be through the T2 copper site, and also that the addition of nitrite to ascorbate-reduced *Sm*Nir produces NO, as occurs using dithionite as the sole electron donor (see Section 3.3).

3.3. Kinetic assays

The pH dependence of Nir activity showed a maximum at pH ~5, similar to that evaluated for Nirs from *A. xylosoxidans* [28], *A. faecalis* [38], and *R. sphaeroides* [39]. Kinetic studies showed that *Sm*Nir

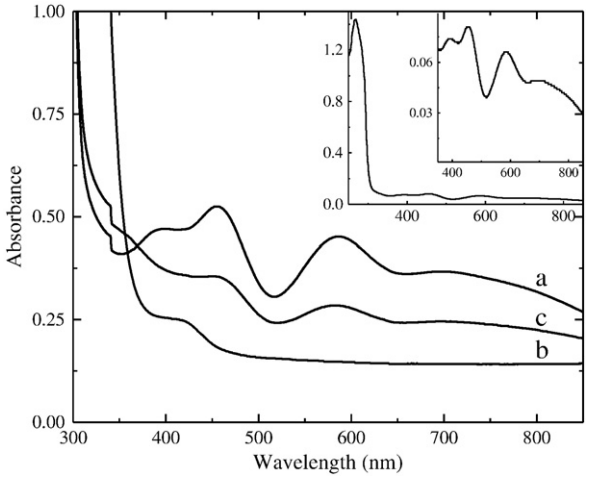

Fig. 3. UV–vis spectra of *Sm*Nir. a) as-purified, b) dithionite-reduced, c) nitrite-reoxidized. Ascorbate reduction yielded a spectrum similar to spectrum "b" (not shown). Spectra "c" and "b" were obtained under anaerobic conditions. Protein concentration ~60 μM trimeric protein in 100 mM Tris–HCl buffer pH 7.1. Dithionite and nitrite concentrations were approximately 20 mM each. The insets show the whole UV–vis absorption spectrum of *Sm*Nir 9 μM.

follows a Mich**aelis–Men**ten mechanism with kinetic parameters $K_m = 0.55 \pm 0.06$ mM NO_2^-, $V_m = 89 \pm 3$ U mg^{-1} and $k_{cat} = 178 \pm 2\ s^{-1}$. Similar K_m-values were reported for the green Nirs from *A. cycloclastes* and *A. faecalis* [1]. Inhibition assays showed that cyanide is an efficient inhibitor, since a remnant of 22% of activity was detected after cyanide addition. No inhibition was observed for nitrate, ammonium, and azide.

To evaluate if the initial interaction T2-nitrite is performed with the enzyme in its oxidized or reduced form, enzyme activity assays were performed with the continuous spectrophotometric method. The kinetic studies initiated upon dithionite addition to nitrite-reacted *Sm*Nir together with EPR studies described in Section 3.4 show that nitrite can bind the Cu(II) T2 center, whereas the kinetic assay with the reduced Nir proves that the nitrite can bind the Cu(I) T2 center. The test initiated with the oxidized enzyme showed a 34% higher activity than that with the reduced enzyme. Kinetic studies complemented with electrochemical experiments performed on *A. faecalis S-6* Nir demonstrated that the enzyme employs a random-sequential mechanism in which at low nitrite concentration electron transfer T1 → T2 occurs prior to nitrite binding, whereas at higher nitrite concentrations, nitrite binding occurs first [15]. Spectroscopic and computational studies of *R. sphaeroides* Nir presented evidence that nitrite binding to the Cu(II) T2 center precedes reduction of this center to Cu(I) [16]. Our results indicate that, though with different efficiency, nitrite binds the T2 center in both Cu(II) and Cu(I) oxidation states.

3.4. EPR characterization of the copper centers

EPR spectra of *Sm*Nir obtained under different experimental conditions are presented in Fig. 4. The spectrum of the as-purified form of *Sm*Nir exhibits two magnetically different components associated with T1 and T2 centers (Fig. 4, spectrum a). The T1 center is completely reduced after ascorbate addition, and becomes EPR silent, whereas the T2 component remains partially in the oxidized form (Fig. 4, spectrum b). This fact indicates that the redox potential of T1 is higher than that of T2, as observed for Nir from *P. chlororaphis* DSM 50135 and *R. sphaeroides* [37,40]. EPR parameters of ascorbate-reduced *Sm*Nir obtained by simulation (see Table in Supplementary Material) indicate an axial spectrum ($g_{//} = 2.304$, $g_{\perp} = 2.053$) with resolved hyperfine structure with the copper nucleus ($I = 3/2$) in the $g_{//}$ region ($A_{//} = 14$ mT), typical of T2 centers. No hyperfine structure associated with the N-histidine atoms coordinating T2 copper site was detected. Simulation of the spectrum of the as-purified form (Fig. 4, spectrum a) using the values obtained for the T2 copper site, allowed us to evaluate $g_z = 2.190$, $g_y = 2.062$, $g_x = 2.033$, $A_z = 5.8$ mT for the T1 center (simulation was performed assuming a 1:1 ratio, see Fig. S1 in Supplementary Material). EPR spectra of both T1 and T2 centers are consistent with a dx2-y2 ground state, with $g_{//} > g_{\perp} > 2$. The T2:T1 ratio assumed in the simulation of spectrum a is in line with the metal analysis, and also indicates that T1 is completely oxidized under aerobic conditions.

Reduction with excess dithionite of the as-purified enzyme under anaerobic conditions produces an EPR-silent form (Fig. 4, spectrum c). Reoxidation of this form under anaerobic conditions with nitrite (nitrite/dithionite ratio ~1:1) yielded a Cu(II) spectrum similar to that of the as-purified enzyme, in line with the corresponding UV–vis data (Fig. 3), but with some extra features at g ~2 (Fig. 4, spectrum d). Spectrum d resembles that observed in *A. faecalis S-6* Nir upon reaction of ascorbate-reduced Nir with NO [41], which was assigned to a side-on Cu^{II}-NO^- species at the T2 site. This interpretation was based on EPR simulations assuming typical g- and A-values for a T2 site plus hyperfine coupling to four N-nuclei at $g_{\perp}$, three from the coordinating histidines and one from the NO, and on X-ray data which showed a side-on NO coordinated to Cu [41]. In contrast, other authors, on the basis of EPR, ENDOR (Electron-Nuclear Double Resonance), and DFT (Density Functional Theory) calculations in *R. sphaeroides* NiR [42,43], concluded that the species generated in solution of ascorbate-reduced Nir with excess NO corresponds to a Cu^{II}-NO_2^- species.

In order to obtain further information on the nitrite/NO-T2 interaction when ascorbate is used as reductant, we performed EPR experiments of *Sm*Nir upon nitrite and NO addition. Nitrite addition to as-purified *Sm*Nir modified slightly the $A_{//}$-value (13.5 mT) with no modifications of the T1 EPR signal (Fig. 4, spectrum e), which indicates that nitrite reacts with the Cu(II) ion of the T2 center. This result is similar to that found in *R. sphaeroides* Nir, which was attributed to the formation of a Cu^{II}-NO_2^- species [44]. Ascorbate addition to nitrite-reacted *Sm*Nir yielded additional modifications of the T2 EPR signal, lowering the $A_{//}$-value to 11.2 mT (Fig. 4, spectrum f). Furthermore, a second rhombic slow relaxing radical-type EPR signal ($g_1 = 2.014$, $g_2 = 2.032$, $g_3 = 2.056$, see inset on Fig. 4), superimposed to the Cu(II) EPR signal, is observed. A similar EPR spectrum was obtained when nitrite was added to a previously ascorbate-reduced *Sm*Nir (see Fig. S2 in Supplementary Material), which indicates that the radical species is not associated with oxidized copper centers. Note also that the resonance positions of this radical-type signal coincide with the features observed at g ~2 in spectrum d when nitrite is added to dithionite-reduced *Sm*Nir, suggesting that the same radical species is generated when dithionite is used as electron donor. The same signal was also obtained upon adding exogenous NO to ascorbate-reduced *Sm*Nir (see Fig. S2 in Supplementary Material),

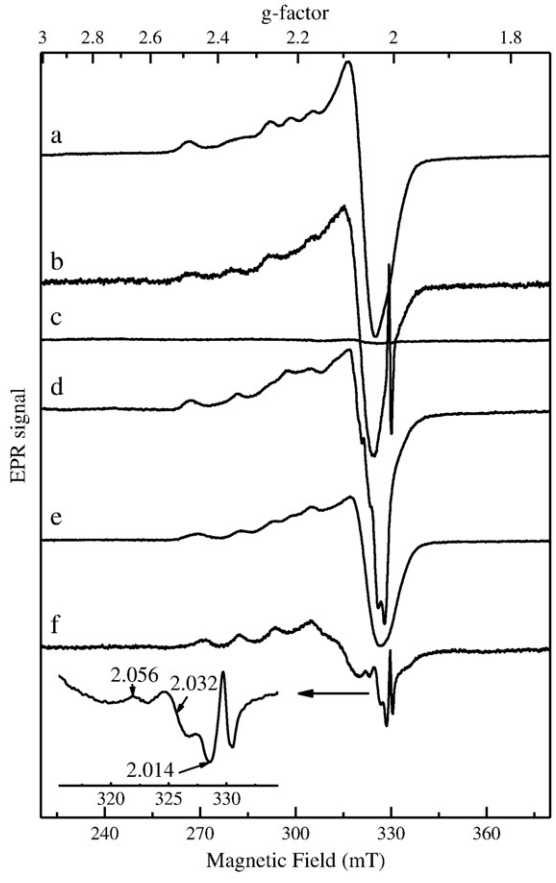

Fig. 4. EPR spectra of *Sm*Nir. a) as-purified, b) ascorbate-reduced, c) dithionite-reduced, d) nitrite-reoxidized, e) as-purified + nitrite, f) as-purified + nitrite + ascorbate. The nitrite-reoxidized form was obtained by brief incubation of the dithionite-reduced-form with substrate under anaerobic conditions. Protein concentration ~150 μM trimeric protein in 100 mM Tris–HCl buffer pH 7.1. The narrow signal at ~330 mT in spectra b and f corresponds to the EPR detectable ascorbyl radical present in the ascorbate solution. Ascorbate, dithionite, and nitrite concentrations were approximately 50 mM each. The inset shows in detail the signal assigned to a Cu(I)-NO species. EPR parameters are given in the text.

confirming that the radical-type signal is a product of the interaction between NO and the T2 copper center. EPR experiments performed on ascorbate-reduced *Sm*Nir reacted with ^{15}N-labeled sodium nitrite (Isotec, 98%) yielded a similar spectrum to that obtained using nitrite with normal isotope composition (see Fig. S2 in Supplementary Material), a fact that indicates that the features observed in the EPR signal cannot be attributed to interaction between the S = 1/2 radical species and the nuclear spin of the N atom of nitrite.

The formation of copper(I)-nitrosyl adducts has been reported in a few copper complexes [45,46] and in the Nirs from *A. faecalis S6* [41], *R. sphaeroides* [42], and *A. cycloclastes* [47]. The crystal structure of *A. faecalis S6* Nir obtained by soaking ascorbate-reduced single crystals with NO-saturated buffer and that of as-isolated *A. cycloclastes* Nir with an endogenous NO ligand showed an unexpected side-on coordination of NO to Cu(I), in contrast to the end-on configuration adopted by NO in copper inorganic complexes [46]. Distinct DFT studies showed that interactions with amino acid side chains are responsible for causing the unusual side-on orientation in Nirs [46,48–51]. Copper-nitrosyl adducts present S = 1/2 ground state associated with nearly axial EPR signals (g_{iso} ~2) and with fast relaxing behavior [46]. These signals are additionally split by hyperfine interaction with the Cu(I) nucleus and the N atom from the NO moiety. The radical-type signal observed by us in *Sm*Nir (Fig. 4, spectrum f), undoubtedly generated from the interaction between T2 and NO, was never observed in Cu-Nirs and is tentatively assigned to a Cu^{I}-$NO^{\bullet}$ species, as NO is highly reactive towards metal centers. This signal cannot be related to either free NO (no EPR resonances were detected for a solution of NO in 100 mM Tris–HCl buffer pH 7.1) or a protein-based radical as its g-values considerably depart from those reported for radicals in proteins [52]. The slow relaxation behavior of the Cu^{I}-$NO^{\bullet}$ species in *Sm*Nir and the lack of detectable hyperfine structure with the N atom from nitrite and the T2 center would indicate a different electronic configuration with respect to the above mentioned copper-nitrosyl adducts.

4. Conclusions

A recombinant copper-containing Nir from *Sinorhizobium meliloti* 2011 was cloned, overexpressed, purified, and characterized for the first time. The spectroscopic and molecular properties of the enzyme indicate that *Sm*Nir is a green Nir with trimeric structure similar to other Nirs obtained from other bacteria. The UV–vis and EPR studies showed that the behavior of the copper centers towards nitrite or reductants such as ascorbate and dithionite are similar to those observed in other Nirs. Nevertheless, a significant difference is found when reduced *Sm*Nir reacts with its own nitrite-produced NO or with exogenous NO. The product of this reaction yields a rhombic radical-type EPR signal never observed in Cu-Nirs, assigned to a Cu^{I}-$NO^{\bullet}$ species. This result shows that closely related copper-containing Nirs from different denitrifying organisms originate distinct radical species during nitrite reduction.

5. Abbreviations

Nir	Copper-containing Nitrite reductase
Sm	*Sinorhizobium meliloti* 2011
IPTG	Isopropyl-β-D-1-thiogalactopyranoside
PCR	Polymerase Chain Reaction
ENDOR	Electron-Nuclear Double Resonance
DFT	Density Functional Theory

Acknowledgments

The *Sinorhizobium meliloti* 2011 strain was kindly provided by A. Lagares (UNLP). Work was supported by projects PICT 2006-00439, CONICET PIP 112-2000801-01079, and CAI + D-UNL. C.D.B and S.A.G are members of CONICET, Argentina.

Appendix A. Supplementary data

Supplementary data to this article can be found online at http://dx.doi.org/10.1016/j.jinorgbio.2012.04.016.

References

[1] W. Zumft, Microbiol. Mol. Biol. Rev. 61 (1997) 533–616.
[2] D.J. Richardson, N.J. Watmough, Curr. Opin. Chem. Biol. 3 (1999) 207–219.
[3] J.P.W. Young, Plant Soil 186 (1996) 45–52.
[4] J.N. Galloway, A.R. Townsend, J.W. Erisman, M. Bekunda, Z. Cai, J.R. Freney, L.A. Martinelli, S.P. Seitzinger, M.A. Sutton, Science 320 (2008) 889–892.
[5] N. Gruber, J.N. Galloway, Nature 451 (2008) 293–296.
[6] V.P. Aneja, W.H. Schlesinger, J.W. Erisman, Nat. Geosci. 1 (2008) 409–411.
[7] B.A. Averill, Chem. Rev. 96 (1996) 2951–2964.
[8] J.W. Godden, S. Turley, D.C. Teller, E.T. Adman, M.Y. Liu, W.J. Payne, J. LeGall, Science 253 (1991) 438–442.
[9] M. Kukimoto, M. Nishiyama, M.E.P. Murphy, S. Turley, E.T. Adman, S. Horinouchi, T. Beppu, Biochemistry 33 (1994) 5246–5252.
[10] T. Inoue, M. Gotowda, Deligeer, K. Kataoka, K. Yamaguchi, S. Suzuki, H. Watanabe, M. Gohow, Y. Kai, J. Biochem. 124 (1998) 876–879.
[11] F.E. Dodd, J. Van Beeumen, R.R. Eady, S.S. Hasnain, J. Mol. Biol. 282 (1998) 369–382.
[12] L.B. LaCroix, S.E. Shadle, Y. Wang, B.A. Averill, B. Hedman, K.O. Hodgson, E.I. Solomon, J. Am. Chem. Soc. 118 (1996) 7755–7768.
[13] S. Suzuki, T. Kohzuma, Deligeer, K. Yamaguchi, N. Nakamura, S. Shidara, K. Kobayashi, S. Tagawa, J. Am. Chem. Soc. 116 (1994) 11145–11146.
[14] E. Libby, B.A. Averill, Biochem. Biophys. Res. Commun. 187 (1992) 1529–1535.
[15] H.J. Wijma, L.J.C. Jeuken, M.P. Verbeet, F.A. Armstrong, G.W. Canters, J. Biol. Chem. 281 (2006) 16340–16346.
[16] S. Ghosh, A. Dey, Y. Sun, C.P. Scholes, E.I. Solomon, J. Am. Chem. Soc. 131 (2009) 277–288.
[17] T.M. Finan, S. Weidner, K. Wong, J. Buhrmester, P. Chain, F.J. Vorhölter, I. Hernandez-Lucas, A. Becker, A. Cowie, J. Gouzy, B. Golding, A. Pühler, Proc. Natl. Acad. Sci. U. S. A. 98 (2001) 9889–9894.
[18] D. Capela, F. Barloy-Hubler, J. Gouzy, G. Bothe, F. Ampe, J. Batut, P. Boistard, A. Becker, M. Boutry, E. Cadieu, S. Dréano, S. Gloux, T. Godrie, A. Goffeau, D. Kahn, E. Kiss, V. Lelaure, D. Masuy, T. Pohl, D. Portetelle, A. Pühler, B. Purnelle, U. Ramsperger, C. Renard, P. Thébault, M. Vandenbol, S. Weidner, F. Galibert, Proc. Natl. Acad. Sci. U. S. A. 98 (2001) 9877–9882.
[19] M.J. Barnett, R.F. Fisher, T. Jones, C. Komp, A.P. Abola, F. Barloy-Hubler, L. Bowser, D. Capela, F. Galibert, J. Gouzy, M. Gurjal, A. Hong, L. Huizar, R.W. Hyman, D. Kahn, M.L. Kahn, S. Kalman, D.H. Keating, C. Palm, M.C. Peck, R. Surzycki, D.H. Wells, K.-C. Yeh, R.W. Davis, N.A. Federspiel, S.R. Long, Proc. Natl. Acad. Sci. U. S. A. 98 (2001) 9883–9888.
[20] F.M. Perrine, C.H. Hocart, M.F. Hynes, B.G. Rolfe, Environ. Microbiol. 7 (2005) 1826–1838.
[21] F. Sanger, S. Nicklen, A.R. Coulson, Proc. Natl. Acad. Sci. U. S. A. 74 (1977) 5463–5467.
[22] F.M. Ferroni, M.G. Rivas, A.C. Rizzi, M.E. Lucca, N.I. Perotti, C.D. Brondino, Biometals 24 (2011) 891–902.
[23] M.M. Bradford, Anal. Biochem. 72 (1976) 248–254.
[24] U.K. Laemmli, Nature 227 (1970) 680–685.
[25] H.D. Niall, C.H.W. Hirs, S.N. Timasheff, Methods Enzymol. 27 (1973) 942–1010.
[26] S. Ida, J. Biochem. 82 (1977) 915–918.
[27] F.D. Snell, C.T. Snell, Colorimetric methods of analysis, including some turbidimetric and nephelometric methods, third ed. D. Van Nostrand Co., New York, 1948.
[28] Z.H. Abraham, B.E. Smith, B.D. Howes, D.J. Lowe, R.R. Eady, Biochem. J. 324 (1997) 511–516.
[29] M. Prudêncio, R.R. Eady, G. Sawers, Biochem. J. 353 (2001) 259–266.
[30] S. Stoll, A. Schweiger, J. Magn. Reson. 178 (2006) 42–55.
[31] P. Wojciech, M.D.J.D. Nicholas, Biochim. Biophys. Acta 828 (1985) 130–137.
[32] G. Denariaz, W. Jackson Payne, J. LeGall, Biochim. Biophys. Acta 1056 (1991) 225–232.
[33] H. Nielsen, J. Engelbrecht, S. Brunak, G. von Heijne, Int. J. Neural Syst. 8 (1997) 581–599.
[34] J.D. Bendtsen, H. Nielsen, G. Von Heijne, S. Brunak, J. Mol. Biol. 340 (2004) 783–795.
[35] M. Prudêncio, R.R. Eady, G. Sawers, J. Bacteriol. 181 (1999) 2323–2329.
[36] Z.H. Abraham, D.J. Lowe, B.E. Smith, Biochem. J. 295 (1993) 587–593.
[37] K. Olesen, A. Veselov, Y. Zhao, Y. Wang, B. Danner, C.P. Scholes, J.P. Shapleigh, Biochemistry 37 (1998) 6086–6094.
[38] T. Kakutani, H. Watanabe, K. Arima, T. Beppu, J. Biochem. 89 (1981) 463–472.
[39] F. Jacobson, A. Pistorius, D. Farkas, W. De Grip, Ö. Hansson, L. Sjölin, R. Neutze, J. Biol. Chem. 282 (2007) 6347–6355.
[40] D. Pinho, S. Besson, C.D. Brondino, E. Pereira, B. de Castro, I. Moura, J. Inorg. Biochem. 98 (2004) 276–286.
[41] E.I. Tocheva, F.I. Rosell, A.G. Mauk, M.E.P. Murphy, Science 304 (2004) 867–870.
[42] O.M. Usov, Y. Sun, V.M. Grigoryants, J.P. Shapleigh, C.P. Scholes, J. Am. Chem. Soc. 128 (2006) 13102–13111.
[43] S. Ghosh, A. Dey, O.M. Usov, Y. Sun, V.M. Grigoryants, C.P. Scholes, E.I. Solomon, J. Am. Chem. Soc. 129 (2007) 10310–10311.
[44] A. Veselov, K. Olesen, A. Sienkiewicz, J.P. Shapleigh, C.P. Scholes, Biochemistry 37 (1998) 6095–6105.

[45] C.E. Ruggiero, S.M. Carrier, W.E. Antholine, J.W. Whittaker, C.J. Cramer, W.B. Tolman, J. Am. Chem. Soc. 115 (1993) 11285–11298.
[46] K. Fujisawa, A. Tateda, Y. Miyashita, K.-i. Okamoto, F. Paulat, V.K.K. Praneeth, A. Merkle, N. Lehnert, J. Am. Chem. Soc. 130 (2008) 1205–1213.
[47] S.V. Antonyuk, R.W. Strange, G. Sawers, R.R. Eady, S.S. Hasnain, Proc. Natl. Acad. Sci. U. S. A. 102 (2005) 12041–12046.
[48] I.H. Wasbotten, A. Ghosh, J. Am. Chem. Soc. 127 (2005) 15384–15385.
[49] G. Periyasamy, M. Sundararajan, I.H. Hillier, N.A. Burton, J.J.W. McDouall, Phys. Chem. Chem. Phys. 9 (2007) 2498–2506.
[50] A.C. Merkle, N. Lehnert, Inorg. Chem. 48 (2009) 11504–11506.
[51] M. Sundararajan, R. Surendran, I.H. Hillier, Chem. Phys. Lett. 418 (2006) 96–99.
[52] A. Ivancich, C. Jakopitsch, M. Auer, S. Un, C. Obinger, J. Am. Chem. Soc. 125 (2003) 14093–14102.
[53] J.D. Thompson, D.G. Higgins, T.J. Gibson, Nucleic Acids Res. 22 (1994) 4673–4680.